ACS Sustainable Chemistry & Engineering

Research Article

Cite This: ACS Sustainable Chem. Eng. 2018, 6, 6203−6210

pubs.acs.org/journal/ascecg

Synthesis of Silicon Nanoparticles from Rice Husk and their Use as Sustainable Fluorophores for White Light Emission

Sandeep Bose, Mohd. Azhardin Ganayee, Biswajit Mondal, Avijit Baidya, Sudhakar Chennu, Jyoti Sarita Mohanty, and Thalappil Pradeep*

DST Unit of Nanoscience (DST UNS) and Thematic Unit of Excellence (TUE), Department of Chemistry, Indian Institute of Technology Madras, Chennai−600 036, India

Supporting Information

ABSTRACT: Silicon nanoparticles (Si NPs) exhibiting observable luminescence have many electronic, optical, and biological applications. Owing to reduced toxicity, they can be used as cheap and environmentally friendly alternatives for cadmium containing quantum dots, organic dyes, and rare earth-based expensive phosphors. Here, we report an inexpensive silicon precursor, namely rice husk, which has been employed for the synthesis of Si NPs by rapid microwave heating. The Si NPs of ∼4.9 nm diameter exhibit observable green luminescence with a quantum yield of ∼60%. They show robust storage stability and photostability and have constant luminescence during long-term UV irradiation extending over 48 h, in contrast to other luminescent materials such as quantum dots and organic dyes which quenched their emission over this time window. Green luminescent Si NPs upon mixing with synthesized red and blue luminescent Si NP species are shown to be useful for energy-efficient white light production. The resulting white light has a color coordinate of (0.31, 0.27) which is close to that of pure white light (0.33, 0.33). The performance of our white light emitting material is comparable to that of a commercial white light emitting diode (WLED) bulb and is shown to be better than that of a commercial compact fluorescent lamp (CFL).

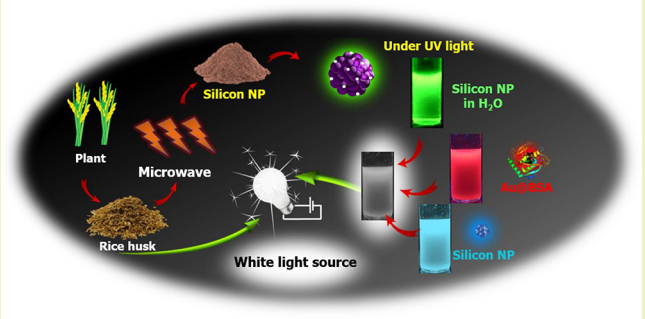

KEYWORDS: *Rice husk, Silicon nanoparticles, Luminescence, Microwave, White light emission*

INTRODUCTION

Silicon as a source of light has been the dream of scientists for several years. Silicon in the thin film form is one of the major foundations of modern society. Until now it has been used as the base material for the development of photovoltaics[1−5] and microelectronics,[6] but silicon emitting light can bring a revolution in photonics,[7] optoelectronics,[8] and biotechnology.[9] In the early 1990s, Canham discovered the emission of visible light from silicon which he attributed to the porous nature of silicon and that finding paved the way for research on luminescent silicon nanoparticles (Si NPs).[10,11] Since then it has been more than two decades of ongoing research which has moved the focus from porous silicon to colloidal Si NPs or silicon quantum dots.[12−21] Printing such thin films require inks based on silicon. Applications of inks composed of Si NPs vary from printable electronics, flexible solar cells, solar roofing, etc. As these particles are biodegradable with an expected environmental lifetime of the order of 6 months with reduced toxicity, they hold great promise in biotechnological applications such as bioimaging[9,22−27] and can be used as a replacement for quantum dots. Production of Si NPs requires high energy processing as silicon exists in nature as SiO_2 which requires energy (ΔH = 169.7 kcal/mol at ∼3000 K for the reaction, $SiO_2 + C = Si + CO_2$) for its reduction.[28] Nanoparticles of silicon are particularly useful to create stable and solvent compatible suspensions. They are also useful due to their inherent changes in the electronic, optical, and mechanical properties. Sustainable manufacturing of Si NPs is important for cheaper, energy efficient, and consequently affordable technologies.

Si NPs have been made chemically by various methods involving chemical reductants. They have also been made by using microwave synthesis,[29] hydrothermal synthesis,[30] chemical vapor deposition,[31] laser ablation,[32] mechanochemical method,[33] plasma assisted aerosol precipitation,[34] sonochemical synthesis,[35] and even room temperature solution phase reduction where the ligand is used for multiple purposes such as capping as well as reduction.[36] All these reactions invariably require costly chemicals, uncommon instrumentation and procedures, harsh experimental conditions, and long time. Most of the time, chemical methods used a few commonly available starting materials such as aminopropyltrimethoxysilane and its variants which are expensive. Si NPs possess weak aqueous solubility due to the presence of hydrophobic groups on the surface (e.g., Si−H bond), and this is a major limitation for their use in biomedical applications. Several methods have

Received: December 28, 2017
Revised: March 5, 2018
Published: March 9, 2018

DOI: 10.1021/acssuschemeng.7b04911
ACS Sustainable Chem. Eng. 2018, 6, 6203−6210

been reported for Si NPs functionalization with hydrophilic groups but functionalization often leads to decrease in quantum yield.[37] Again, synthesis involves the top-down method where precursors, such as silicon powder, SiO_x, nanowires, etc., were used. Below we present a bottom-up approach for the synthesis of hydrophilic Si NPs preserving high quantum yield.

Rice husk as a resource is estimated to be available to the extent of 770 million tons annually, which is generally used as a heat source in rice mills and hence readily available. Our method uses a simple, one-pot, rapid microwave reduction of silicon precursors in the husk presumably by carbon precursors under conditions of ambient pressure and high temperature, available in a microwave. The particles are stable at room temperature and at different experimental conditions for an extended period of time allowing them to be useful for applications.

EXPERIMENTAL SECTION

Materials. Rice grains were purchased from a local market in Chennai (Tamil Nadu, India). Sodium hydroxide was purchased from Merck Life Science Private Ltd. CdTe (Red luminescent) quantum dot sample was a gift from Prof. E. Prasad's lab (Dept. of Chemistry, IIT Madras). For preparing solutions, Milli-Q (Millipore) water was used as the solvent. Perylene dye was purchased from Sigma-Aldrich for quantum yield calculations. Aminopropyl trimethoxysilane (APTMS) was purchased from Sigma-Aldrich and was used for the synthesis of blue Si NPs. For the synthesis of Au@BSA, both $HAuCl_4$ and the protein, bovine serum albumin (BSA), were purchased from Sigma-Aldrich.

Synthesis of Green Luminescent Si NPs. About 2 g of rice husk were ground to make a fine powder. To that powder, about 10 mL of aqueous NaOH (1M) was added. No additional reducing and protecting agents were added to it. This mixture was heated in a microwave oven (2.45 GHz, 600 W). During the reaction, as the solution was dried, 5 mL of solvent was added and heated and the process was continued for 1 h at an interval of 10 min. Finally, the microwaved solution was taken out and centrifuged to remove any unreacted materials present. The supernatant was collected and analyzed, and it was found to contain Si NPs.

Removal of Anthocyanin Dye from Si NPs. Rice grains contain pigments like anthocyanin which in basic medium shows green luminescence. Removal of anthocyanin from the Si NPs was necessary to make sure that the observed luminescence was due to Si NPs and not due to anthocyanin. The separation was done using Amicon Ultra-15 Centrifugal Filter Units, with a molecular weight cutoff of 10 kDa. As the molecular weight of Si NPs was different from anthocyanin, they were easily separated. To remove any adsorbed anthocyanin, the particles were washed repeatedly.

Quantum Yield Calculation of Si NPs. For the green luminescent Si NPs, the PL quantum yield was calculated using perylene dye as a reference, taken in cyclohexane. Freshly prepared solution was used to avoid errors. Perylene has excitation and emission maxima in the range of 360−420 and 430−530 nm, respectively. For comparison with Si NPs, the excitation wavelength chosen was 420 nm. At this excitation wavelength, the optical densities of both the dye and Si NPs were adjusted to the same values. Photoluminescence (PL) spectra of the solutions of the same optical density solutions were recorded and areas of the PL curves were calculated. Integrated PL intensities vs corresponding optical densities were plotted and fitted with a straight line to yield two slopes which could be employed in determining the quantitative output using the established equation:

$$\Phi_{Si} = \Phi_{Dye}(K_{Si}/K_{Dye})(RI)_{Si}^{2}/(RI)_{Dye}^{2}$$

where K_{Si} and K_{Dye} stand for straight line slopes and $(RI)_{Si}$, $(RI)_{Dye}$, Φ_{Si}, and Φ_{Dye} represent the refractive indices of the solvents and quantum yields of the Si NPs and the dye, respectively.[38]

Comparison of Photostability of Fluorescein Isothiocyanate Dye, CdTe Quantum Dots, and Si NPs. For the photostability comparison, the PL intensities of all the luminescent materials were adjusted to the same value. Equal volumes of all the samples were taken for better comparison. The measurements were performed under a 365 nm UV lamp with a power of 6 W.

pH Stability and Time-Dependent Stability of Si NPs. pH values of the silicon nanoparticle solutions were adjusted by adding aq NaOH and HCl dropwise. A digital pH meter (MP-1 PLUS, Susima technologies) was used for the measurement of pH of the solution. Fluorescence intensities of the samples were measured using Horiba Yvon Nanolog (FL-1000) fluorimeter. Time-dependent luminescence intensity measurements were performed over a period of 1 month to check the stability of the nanoparticles. The measurements were performed at an interval of 3 days.

White Light Emission. A mixture of green Si NPs (rice husk synthesized), blue luminescent Si NPs (APTMS synthesized), and red luminescent Au@BSA clusters were prepared to demonstrate white light emission. The materials were selected such that they all show emission at the given excitation range as well as they are soluble in the same solvent, i.e. water. The excitation wavelength chosen was 360 nm.

Synthesis of Blue Emitting Si NPs. About 0.8 g of sodium citrate was dissolved in 20 mL of water. To this solution, 1 mL of aminopropyl trimethoxysilane (APTMS) was added and agitated homogeneously for 2 min. Then the solution was transferred into a hydrothermal bomb and was kept at 170 °C for 24 h and cooled to room temperature. The transparent solution was dialyzed using a membrane with molecular weight cut off 12 kDa and stored at 4 °C for use.

Synthesis of Au@BSA Cluster. A 10 mL portion of the aqueous solution of $HAuCl_4$ (6 mM) was added to 10 mL of BSA (25 mg/mL). The solution was stirred for 5 min, and 1 mL of NaOH (1M) was subsequently added. The pH of the solution was kept at 12. The reaction was continued with mild stirring for 24 h. The color of the solution changed from golden yellow to dark orange. The solution exhibits intense luminescence under UV light. The sample was dialyzed using a membrane with molecular weight cut off 12 kDa, and the purified sample was kept at 4 °C for further use.

Luminous Efficacy Measurements of CFL, WLED, and Our Material. A compact fluorescent lamp (CFL) and white light emitting diode (WLED) of power 14 and 5 W, respectively were bought for the luminous flux comparison. The luminous flux of the emitting material was given as, luminous flux (ϕ_v) = illuminance (E_v) × surface area (A).

For easier calculation of the surface area, a spherical CFL and a WLED were purchased. Surface area of CFL and WLED are $4\pi r^2$ where r is the radius of the spherical bulbs. Surface areas of cylindrical Petri dish on which our material was coated is $2\pi rh + \pi r^2$. The illuminance was measured using a Lux meter. Luminous efficacy was calculated as luminous flux per unit power. For the illuminance measurement, the distance from the source to the Lux meter sensor was kept constant. A (3 W, 3 V) UV LED was used as the source for white light emission.

RESULTS AND DISCUSSION

Synthesis, Mechanism, and Optical Properties of Si NPs. Synthesis of silica nanoparticles from rice husk biomass is an established area both in research and in industry. Such materials are considered as a sustainable source of high quality silica for diverse applications.[39−41] There are previous reports on the synthesis of porous silica particles by microwave irradiation of chemically process rice husk.[42] Reports are also available on the magneisothermic reduction of silica to silicon which was utilized as an electrode material.[43] Both these methods do not report synthesis of luminescent Si NPs. Our synthetic methodology does not utilize prior chemical processing and avoid the use of external reducing agent.

DOI: 10.1021/acssuschemeng.7b04911
ACS Sustainable Chem. Eng. 2018, 6, 6203−6210

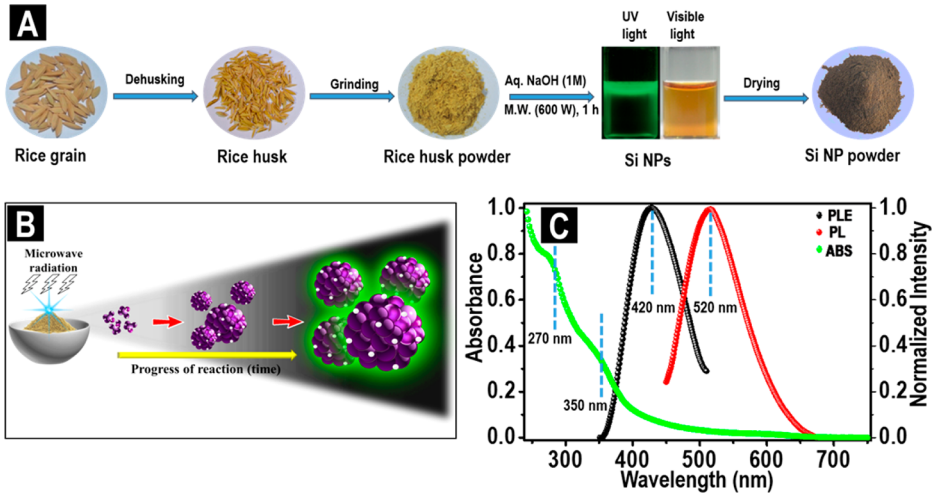

Figure 1. (A) Procedures involved in the synthesis of green luminescent Si NPs. (B) Schematic illustration of nanoparticle nucleation, growth, and coalescence leading to smaller Si NPs. (C) Absorption (ABS), excitation (PLE), and emission spectra (PL) of the Si NPs.

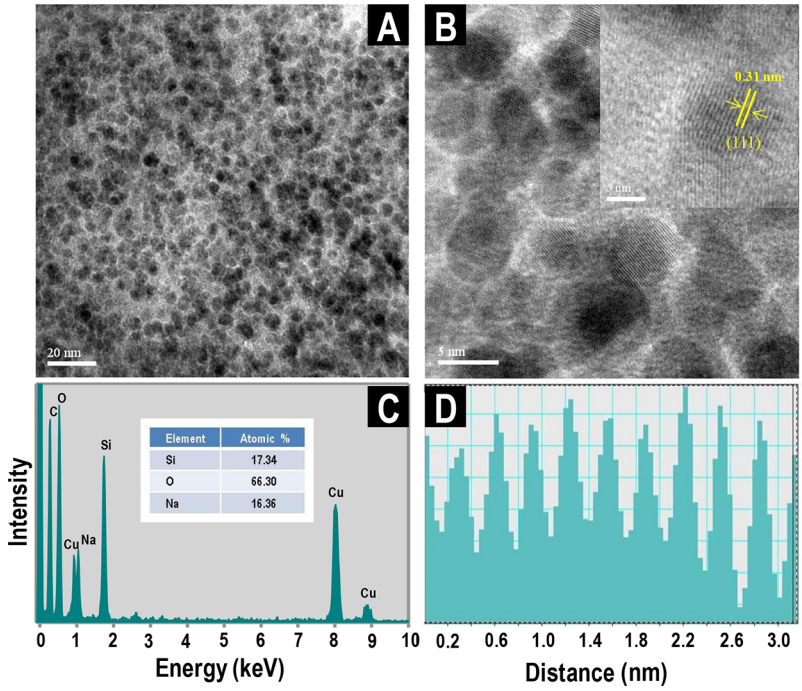

Figure 2. (A) Large area TEM image of the rice husk synthesized Si NPs. (B) HRTEM image of the Si NPs and the inset shows a lattice spacing of 0.31 nm arising from the (111) plane of silicon. (C) EDAX spectrum of Si NPs along with the atomic percentages of the elements present. Carbon and copper are from the grid although some carbon is present in the sample too. (D) Lattice distance profile of Si NPs for the (111) crystal plane. It is the profile of 10 consecutive lattice planes, an average of which was considered as the lattice distance between the planes.

The synthetic procedure used is shown in Figure 1A. Fine powder of husk was taken and 1 M NaOH was added dropwise with stirring. The solution was heated in a microwave oven for an hour in a porcelain crucible. Finally it was taken out and cooled to room temperature and separated from anthocyanin by centrifugal ultrafiltration. The Si NPs were stored at 4 °C for further use. One of the advantages of this method of synthesis of Si NPs is that no additional reducing agent was used for reducing silica to silicon. The reduction was presumably due to the carbon backbone materials (cellulose, hemicellulose, lignin, *etc.*) present in it and the exact mechanism of reduction is not clearly understood. Reduction of silica to silicon by carbon takes place at extremely high temperatures, i.e., at ∼3000 °C which follows the reaction, $SiO_2 + C = Si + CO_2$. Although the temperature employed here is only 170 °C, it is presumably the local temperature around the particles that is attributed to the reduction which can be as high as the reduction temperature of silica.

The growth of Si NPs upon microwave heating may occur via the formation of smaller nuclei followed by Ostwald ripening (Figure 1B). Once a sufficient number of nuclei form, Ostwald ripening occurs by the coalescence of smaller particles onto the larger ones in order to reduce the surface free energy. In our case, microwave heating was performed for 1 h to get the required nanoparticles. Figure 1C displays the normalized UV−vis absorption, excitation as well as photoluminescence of the nanoparticles. The λ_{ex} of these nanoparticles was 420 nm and the emission at the corresponding excitation was 520 nm.

DOI: 10.1021/acssuschemeng.7b04911
ACS Sustainable Chem. Eng. 2018, 6, 6203−6210

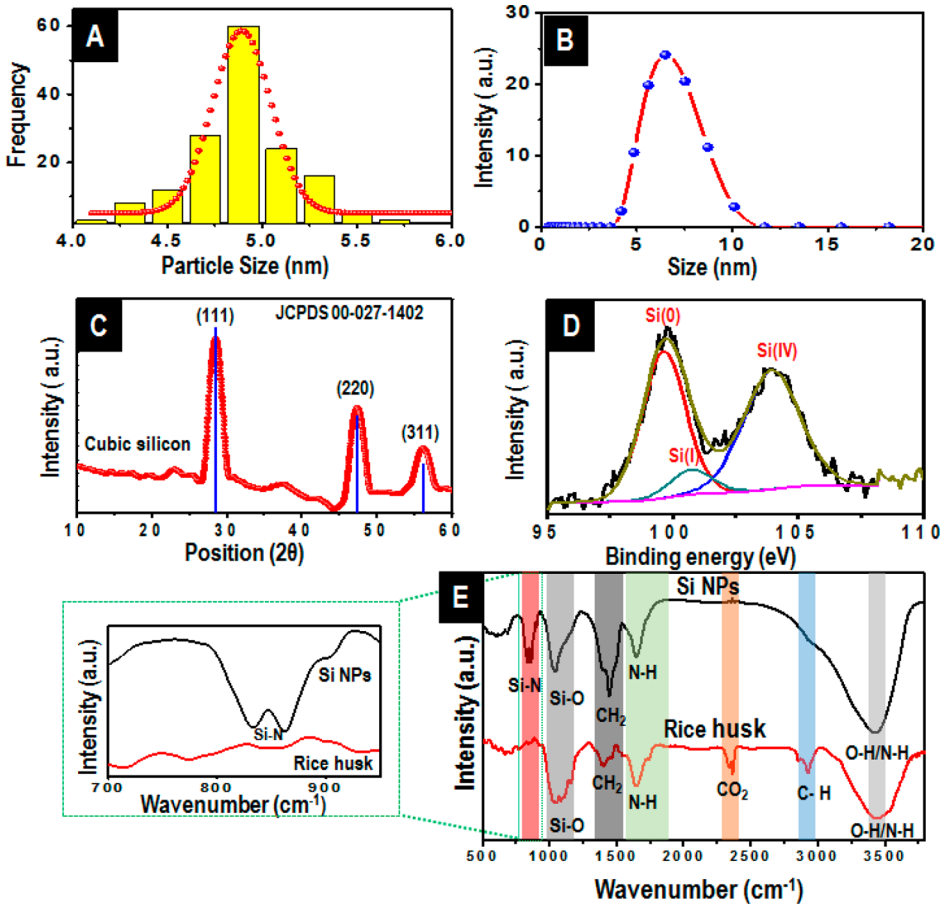

Figure 3. (A) Size distribution of Si NPs from the TEM image with an average size of 4.9 nm. (B) DLS size measurement of green emitting Si NPs shows an average size of 6.5 nm. (C) XRD characterization of the as Si NPs along with the standard JCPDS data for cubic silicon. (D) XPS spectrum of Si NPs showing features of Si(0) due to silicon core and Si(I) due to oxidized silicon surface. The strong main feature at 103.7 eV is due to silica. (E) FTIR spectra of the Si NPs and rice husk with the regions marked showing possible functionalities. Specific region is expanded on the left.

Distinct absorption features of the nanoparticles were observed at 270 and 350 nm. The energy at 350 nm corresponds to the intrinsic direct Γ−Γ band gap of silicon and is a commonly observed peak in Si NPs.[38] Peak at 270 nm corresponds to the L−L transition of silicon.[44] The existence of two peaks gave an indication of the presence of silicon particles in solution. The solution appears brown under white light illumination and exhibits green luminescence under ultraviolet light. The solution upon freeze-drying gave a dark brown powder (Figure 1A). The system has yielded unreacted silica particles also. The silica particles were removed carefully by changing the pH. The estimated yield of Si NPs was 5%.

TEM and EDS Characterization of Si NPs. Figure 2A shows a large area TEM image of Si NPs displaying the high population of nanoparticles formed during the synthesis. Nanoparticles are largely spherical in nature as shown in the HRTEM image (Figure 2B) having a lattice distance of 0.31 nm matching with the (111) plane of cubic silicon. There were no additional reducing agents or protecting ligands added to the solution. The spherical nature of the nanoparticle is an indication of surface protection presumably by the oxygen and nitrogen containing decomposition products of rice husk. EDAX spectrum and lattice distance (Figure 2C and D) profiles further confirm the existence of Si NPs in solution.

Structure and Surface Characterization of Si NPs. The nanoparticles feature excellent hydrophilic nature owing to the nature of surface functionalities. In order to check the dispersibility of Si NPs, organic solvents, i.e. DCM and hexane, were added to the aqueous dispersion (Figure S13A and B) and the mixture was shaken. As organic solvents are nonpolar and hydrophobic in nature, the Si NPs were not dispersible and a separate layer was formed whereas the Si NPs were dispersed in water. Figure 3A showed the size distribution of the nanoparticles and average size of these nanoparticles observed was 4.9 ± 0.2 nm demonstrating their highly monodisperse nature. Additional information on size of the nanoparticles in solution was collected by DLS measurements. The size of the nanoparticle observed was 6.5 nm (Figure 3B), slightly higher than that observed in TEM owing to distinct surface states of Si NPs under different measurement environments (DLS measurements are based on hydrodynamic radius which includes the surface ligands).[16,36,45−47] Zeta potential of the Si NPs were measured to be −27.1 mV. This gives an idea about the groups at the surface of Si NPs which are likely to be composed of O and N containing species.

Figure 3C displays the XRD features of the as synthesized nanoparticles. Standard diffraction peaks at 28.4°, 47.3°, and 56.1° corresponding to (111), (220), and (311) crystallographic planes, respectively, matching with the XRD pattern of cubic silicon. For comparison, JCPDS data of cubic silicon (file no. 00-027-1402) are also presented for reference. Figure 3D shows the XPS spectrum of the synthesized nanoparticles. The deconvoluted spectrum shows the presence of different oxidation states of silicon present in the sample. Peaks at

DOI: 10.1021/acssuschemeng.7b04911
ACS Sustainable Chem. Eng. 2018, 6, 6203−6210

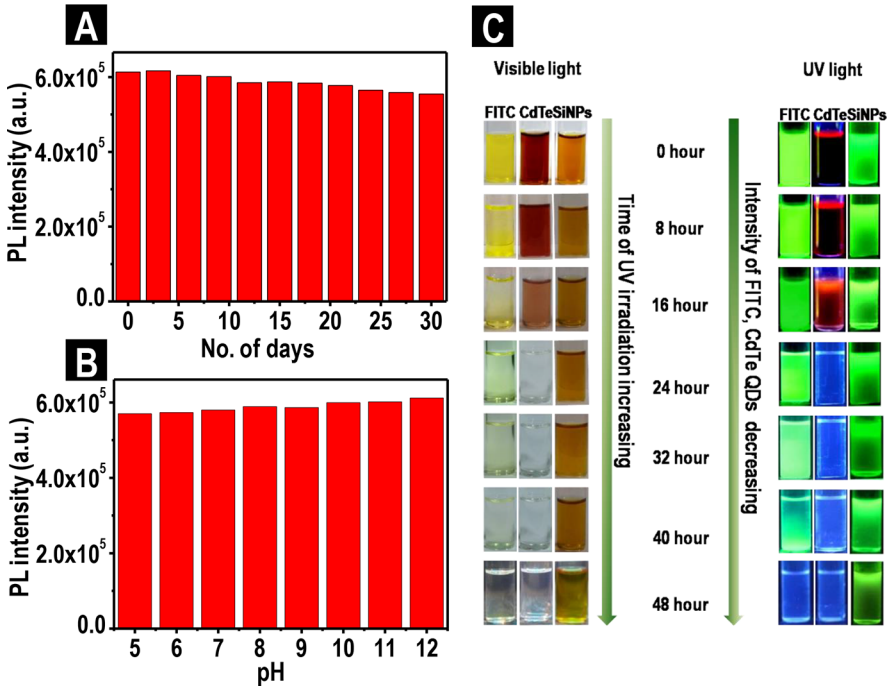

Figure 4. (A) Variation of PL intensity of Si NPs as a function of time. (B) Variation of PL intensity as a function of pH. (C) Photostability comparison and photograph of FITC, CdTe QDs, and Si NPs under continuous UV irradiation up to 48 h.

~99.6, 100.7, and 103.7 eV confirm the presence of Si(0), Si(I), and Si(IV) oxidation states, respectively. The Si(0) state indicates the formation of reduced silicon. The Si(I) state is probably due to surface oxidation by the attachment of oxygen and nitrogen containing species as protecting agents. The oxidation state of (IV) indicates the unreacted silica present in the form of silicates of sodium (NaOH was added). In contrast, the XPS spectrum of rice husk (Figure S7) exhibits two peaks in the energy range of 101 and 103.5 eV, attributed to the suboxides and oxides of silicon (silica), respectively. The XPS data clearly suggest the reduction of Si(IV) to Si(0) in the prepared Si NPs by microwave reduction. In order to acquire molecular information, FTIR spectra (Figure 3F) of the Si NPs were measured along with the precursor rice husk. Rice husk shows a peak at ~3435 cm^{-1} due to the vibrational stretching of N−H/O−H bonds present. Similarly, peaks at 2923, 1645, 1455, and 1405 cm^{-1} correspond to sp^3 C−H stretching, N−H bending, CH_2 bending, and C−N stretching, respectively. Peaks at 2923 and 1455 cm^{-1} indicate the presence of carbon backbone materials like cellulose, hemicelluloses, etc. Peaks at 1645 and 1405 cm^{-1} indicate the presence of amino/amide groups, probably due to the presence of proteins/amino acids present in it. Peaks at 2342 and 2361 cm^{-1} arise due to background CO_2. Peaks at 1040 cm^{-1} correspond to Si−O stretching. In striking contrast, one can clearly see the additional peaks at 833 and 857 cm^{-1} ascribed to the Si−N stretching vibrations in Si NPs confirming the existence of Si−N bonds which are missing in the IR spectrum of rice husk.[47] Similarly, peaks at 1045, 1645, 1445, and 1405 cm^{-1} are due to Si−O, N−H, CH_2, and C−N stretching and bending vibrations, respectively. FTIR characterization gives an idea about the nature of the surface ligands protecting the Si NP core.

pH and Photostability Comparison. Photoluminescence spectrum of Si NPs at an interval of 3 days, for a period of 1 month was studied (Figure S15A). The figure shows that there is no shift in the emission maximum during this period indicating that the Si NPs are quite stable and do not degrade or change with time (Figure 4A). The decrease in intensity from the first day of the measurement and after 30 days is only 12%. Preservation the PL properties for longer period can be effective for bioimaging as well as biosensing. In order to function effectively in biological media, the nanoparticles should be stable over a wide range of pH as different biological systems work under different pH conditions. The fluorescence spectrum as a function of pH was measured (Figure S15B). The pH was varied from 5 to 12 covering the pH range of most microorganisms. Variation in fluorescence intensity (Figure 4B) was within 9% when the pH was changed from basic (pH 12) to acidic environment (pH 5). Si NPs possess excellent photostability under UV-irradiation, preserving its stability as well as brightness. Photostability comparisons were performed among the green luminescent nanoparticles, CdTe quantum dots, and fluorescein isothiocyanate (FITC) dye under UV lamp. Under UV light, CdTe degraded faster; after 24 h, it was completely degraded, whereas the dye quenched owing to photobleaching. The PL intensity of CdTe quantum dots decreased by more than 80% in the first 16 h (Figure S10) and was completely quenched by 24 h. A similar trend was observed in the case of the dye. However, the fluorescence of nanoparticles was intact. There were several methods reported such as biomimetic synthesis of Si NPs where the synthesis was cheap, facile, and green, but the quantum yield obtained was low in the range of 15−20%.[29] Reports of ultra bright luminescent Si NPs having quantum yield up to 90% has been reported, but such methods used are expensive as well as toxic precursors.[43] In contrast, our material is competitive enough with a quantum yield of ~60% (Figure S8) which used an inexpensive precursor.

Si NPs Utilized in White Light Production. Nowadays white light emitting materials have gained significant attention as major components in light emitting devices (LEDs).[48] Taking into consideration the huge energy demand, especially

DOI: 10.1021/acssuschemeng.7b04911
ACS Sustainable Chem. Eng. 2018, 6, 6203−6210

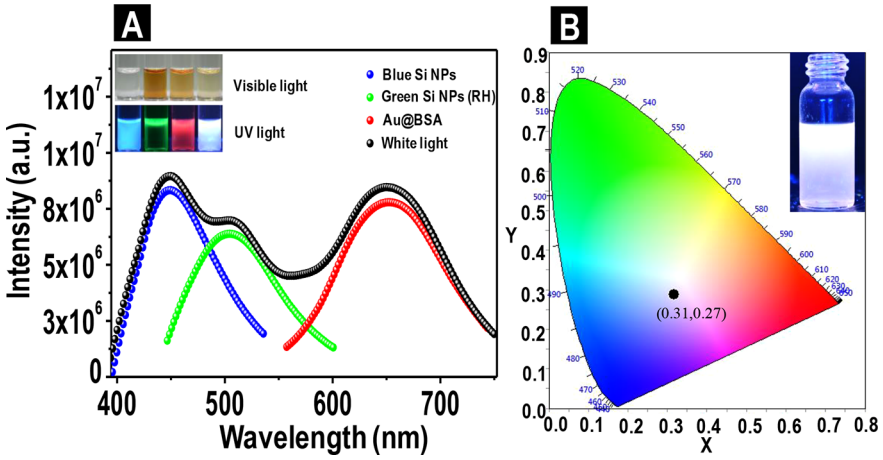

Figure 5. (A) Emission of white light from a mixture of blue (Si NPs), green (RH-Si NPs), and red (Au@BSA) luminescent materials. (inset) Photographs of different luminescent materials under UV and visible light. (B) Chromaticity diagram showing the coordinates of the white light emitted (0.31, 0.27) after mixing the materials.

in developing economies, WLEDs are important for energy saving. Low cost and environment friendly WLEDs utilizing organic and inorganic molecules have attracted huge interest in recent years and can be substitutes for expensive rare-earth based sources or Cd based inorganic quantum dots.[49−51] Herein, the synthesized green luminescent Si NPs were mixed with blue emitting Si NPs and red emitting Au@BSA[52] clusters to produce white light and the performance of the composite material was checked. The inset in Figure 5A shows the individual colors under UV and visible light as well as the white light obtained after mixing the solutions (in a 2:1:1 volume ratio of blue, green, and red luminescent materials). The wavelength selected for excitation was 365 nm. Figure 5A shows the individual PL spectra of the luminescent nanoparticles along with the spectrum of white light emitted from the mixed sample.

The color characteristics from the luminescent materials were analyzed using a CIE 1931 chromaticity diagram. The CIE coordinates observed (Figure 5B) for the white light was (0.31, 0.27) which is in excellent agreement with the pure white light coordinates of (0.33, 0.33).

Application of the White Emitting Material as a Light Source. Luminescence from the material is generally observed in the colloidal phase. Often aggregation induced quenching lowers the luminescence properties when the sample was dried to films or powders.[53,54] However, in order to use the material directly as a phosphor in WLEDs, high quality luminescence from the material in the solid state is needed. In order to check the solid state emission, the material was mixed with cellulose as a supporting material and kept at 60 °C for drying on a Petri dish and its luminescence was checked. A UV LED was purchased, and a Petri dish coated with the material was placed above it. Figure 6A−C are demonstrations of the usability of the materials as a white light source. It displays excellent white light emission in the solid state ensuring its potential application in the field of WLEDs. The performance of our material was compared with the commercial WLEDs and CFLs. Figure 6D shows such a comparison. The luminous efficacy of our material was superior to the commercial CFLs. Temperature-dependent luminescence measurements were performed to check the thermal stability of white light emitting material. It showed negligible change over the measured range of temperatures. The material was not only unaltered to the applied temperature but also was endowed with stability over a longer period of time (Figure S11 and S12) making it suitable as a phosphor material in LEDs.

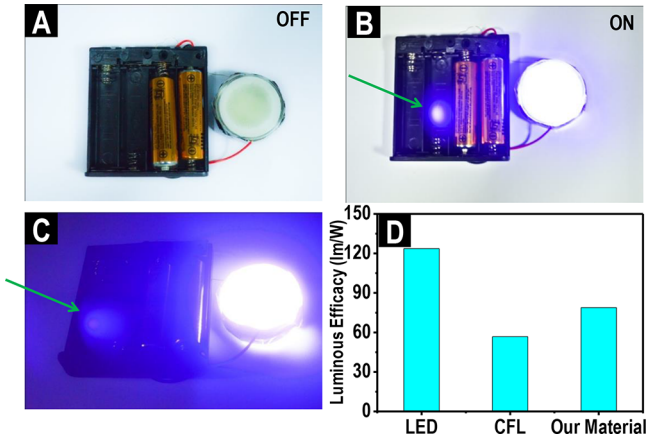

Figure 6. (A) Photographic image of the material coated Petri dish connected to a 3 V, 3 W UV LED when the battery was turned off, under visible light. (B) Photographic image of the same material emitting white light when the battery was turned on under visible light. (C) Photographic image of the material emitting white light when the battery was turned on under dark. A white spot marked with an arrow appeared in B and C due to camera reflection. (D) Luminous efficacy comparison of our material with a commercial WLED and CFL.

CONCLUSION

In summary, we have demonstrated a one-pot solution-processed low temperature synthesis of Si NPs showing bright green emission from a cheap, readily available precursor, namely rice husk without using expensive equipment, harsh conditions, and complicated procedures. The synthetic method is rapid and cost-effective and can be applied for mass production (0.1 g of Si NPs from 2 g of rice husk). The nanoparticles exhibit excellent monodispersity and water dispersibility, high photo- and pH-stability and high quantum yield, and hold promise for a wide range of optoelectronic and bioimaging applications. Owing to their reduced toxicity, they can be employed as alternatives to inorganic quantum dots and organic dyes. The material offers stable solution as well as solid state luminescence, reflecting their capabilities as a sensor and

DOI: 10.1021/acssuschemeng.7b04911
ACS Sustainable Chem. Eng. 2018, 6, 6203−6210

can be utilized as a phosphor material for the production of white LEDs and lasers, thereby extending its applicability for domestic, industrial, and research purposes. Rice husk synthesized Si NPs may facilitate their use for solar cells, biosensors, printable electronics, etc., and may be used in the advancement of nanoparticle-based bioimaging.

■ ASSOCIATED CONTENT

Supporting Information

The Supporting Information is available free of charge on the ACS Publications website at DOI: 10.1021/acssuschemeng.7b04911.

TEM images of the rice husk synthesized Si NPs in the presence of microwave and their absence without microwave; absorption features of Si NPs, anthocyanin, Si NPs + anthocyanin; TEM images of the residue and supernatant after separation using 10 kDa molecular mass cutoff tubes; EDS and elemental mapping of rice husk to show the silica structure; Excitation wavelength-dependent emission spectra of Si NPs; full range XPS spectrum along with O 1s, C 1s, Na 1s spectra of Si NPs; XPS spectra of rice husk sample; data corresponding to quantum yield determinations; TEM images showing the unaltered Si NPs on changing pH; PL data to show photostability of Si NPs; time-dependent white light emission data; temperature-dependent intensity of white light; hydrophilic nature of Si NPs; solid state white light emission of the material and time- and pH-dependent PL of the Si NPs (PDF)

■ AUTHOR INFORMATION

Corresponding Author

*E-mail: pradeep@iitm.ac.in.

ORCID

Avijit Baidya: 0000-0001-5215-2856

Thalappil Pradeep: 0000-0003-3174-534X

Notes

The authors declare no competing financial interest.

■ ACKNOWLEDGMENTS

We thank the department of science and technology, Government of India, for constantly supporting our research program of nanomaterials. S.B., B.M., and J.S.M. thank IIT Madras for their research fellowships. A.B. thanks the DST for a fellowship. M.A.G. thanks the UGC for a fellowship. S.C. thanks the CSIR for a fellowship. We thank Dr. Soumya Sivalingam for providing the CdTe quantum dots.

■ REFERENCES

(1) Savin, H.; Repo, P.; von Gastrow, G.; Ortega, P.; Calle, E.; Garin, M.; Alcubilla, R. Black silicon solar cells with interdigitated back-contacts achieve 22.1% efficiency. *Nat. Nanotechnol.* **2015**, *10*, 624–628.

(2) Oh, J.; Yuan, H.-C.; Branz, H. M. An 18.2%-efficient black-silicon solar cell achieved through control of carrier recombination in nanostructures. *Nat. Nanotechnol.* **2012**, *7*, 743–748.

(3) Jeong, S.; McGehee, M. D.; Cui, Y. All-back-contact ultra-thin silicon nanocone solar cells with 13.7% power conversion efficiency. *Nat. Commun.* **2013**, *4*, 3950.

(4) Toor, F.; Branz, H. M.; Page, M. R.; Jones, K. M.; Yuan, H.-C. Multi-scale surface texture to improve blue response of nanoporous black silicon solar cells. *Appl. Phys. Lett.* **2011**, *99*, 103501.

(5) Tian, B.; Zheng, X.; Kempa, T. J.; Fang, Y.; Yu, N.; Yu, G.; Huang, J.; Lieber, C. M. Coaxial silicon nanowires as solar cells and nanoelectronic power sources. *Nature* **2007**, *449*, 885–889.

(6) Hirschman, K. D.; Tsybeskov, L.; Duttagupta, S. P.; Fauchet, P. M. Silicon-based visible light-emitting devices integrated into micro-electronic circuits. *Nature* **1996**, *384*, 338–341.

(7) Priolo, F.; Gregorkiewicz, T.; Galli, M.; Krauss, T. F. Silicon nanostructures for photonics and photovoltaics. *Nat. Nanotechnol.* **2014**, *9*, 19–32.

(8) Ng, W. L.; Lourenco, M. A.; Gwilliam, R. M.; Ledain, S.; Shao, G.; Homewood, K. P. An efficient room-temperature silicon-based light-emitting diode. *Nature* **2001**, *410*, 192–194.

(9) Park, J.-H.; Gu, L.; von Maltzahn, G.; Ruoslahti, E.; Bhatia, S. N.; Sailor, M. J. Biodegradable luminescent porous silicon nanoparticles for in vivo applications. *Nat. Mater.* **2009**, *8*, 331–336.

(10) Cullis, A. G.; Canham, L. T. Visible light emission due to quantum size effects in highly porous crystalline silicon. *Nature* **1991**, *353*, 335–338.

(11) Canham, L. T. Silicon quantum wire array fabrication by electrochemical and chemical dissolution of wafers. *Appl. Phys. Lett.* **1990**, *57*, 1046–1048.

(12) Pavesi, L.; Dal Negro, L.; Mazzoleni, C.; Franzo, G.; Priolo, F. Optical gain in silicon nanocrystals. *Nature* **2000**, *408*, 440–444.

(13) Ding, Z.; Quinn, B. M.; Haram, S. K.; Pell, L. E.; Korgel, B. A.; Bard, A. J. Electrochemistry and electrogenerated chemiluminescence from silicon nanocrystal quantum dots. *Science* **2002**, *296*, 1293–1297.

(14) Tsybeskov, L.; Lockwood, D. J.; McCaffrey, J. P.; Labbe, H. J.; Fauchet, P. M.; White, B., Jr.; Diener, J.; Kovalev, D.; Koch, F.; Grom, G. F. Ordering and self-organization in nanocrystalline silicon. *Nature* **2000**, *407*, 358–361.

(15) Gu, L.; Hall, D. J.; Qin, Z.; Anglin, E.; Joo, J.; Mooney, D. J.; Howell, S. B.; Sailor, M. J. In vivo time-gated fluorescence imaging with biodegradable luminescent porous silicon nanoparticles. *Nat. Commun.* **2013**, *4*, 3326.

(16) Zhong, Y.; Peng, F.; Wei, X.; Zhou, Y.; Wang, J.; Jiang, X.; Su, Y.; Su, S.; Lee, S.-T.; He, Y. Microwave-Assisted Synthesis of Biofunctional and Fluorescent Silicon Nanoparticles Using Proteins as Hydrophilic Ligands. *Angew. Chem., Int. Ed.* **2012**, *51*, 8485–8489.

(17) Mastronardi, M. L.; Hennrich, F.; Henderson, E. J.; Maier-Flaig, F.; Blum, C.; Reichenbach, J.; Lemmer, U.; Kubel, C.; Wang, D.; Kappes, M. M.; Ozin, G. A. Preparation of Monodisperse Silicon Nanocrystals Using Density Gradient Ultracentrifugation. *J. Am. Chem. Soc.* **2011**, *133*, 11928–11931.

(18) Anthony, R. J.; Cheng, K.-Y.; Holman, Z. C.; Holmes, R. J.; Kortshagen, U. R. An All-Gas-Phase Approach for the Fabrication of Silicon Nanocrystal Light-Emitting Devices. *Nano Lett.* **2012**, *12*, 2822–2825.

(19) Purkait, T. K.; Iqbal, M.; Wahl, M. H.; Gottschling, K.; Gonzalez, C. M.; Islam, M. A.; Veinot, J. G. C. Borane-catalyzed room-temperature hydrosilylation of alkenes/alkynes on silicon nanocrystal surfaces. *J. Am. Chem. Soc.* **2014**, *136*, 17914–17917.

(20) Mastronardi, M. L.; Henderson, E. J.; Puzzo, D. P.; Ozin, G. A. Small Silicon, Big Opportunities: The Development and Future of Colloidally-Stable Monodisperse Silicon Nanocrystals. *Adv. Mater.* **2012**, *24*, 5890–5898.

(21) Ganguly, S.; Kazem, N.; Carter, D.; Kauzlarich, S. M. Colloidal synthesis of an exotic phase of silicon: the BC8 structure. *J. Am. Chem. Soc.* **2014**, *136*, 1296–1299.

(22) Cheng, X.; Lowe, S. B.; Reece, P. J.; Gooding, J. J. Colloidal silicon quantum dots: from preparation to the modification of self-assembled monolayers (SAMs) for bio-applications. *Chem. Soc. Rev.* **2014**, *43*, 2680–2700.

(23) Peng, F.; Su, Y.; Zhong, Y.; Fan, C.; Lee, S.-T.; He, Y. Silicon Nanomaterials Platform for Bioimaging, Biosensing, and Cancer Therapy. *Acc. Chem. Res.* **2014**, *47*, 612–623.

(24) McVey, B. F. P.; Tilley, R. D. Solution Synthesis, Optical Properties, and Bioimaging Applications of Silicon Nanocrystals. *Acc. Chem. Res.* **2014**, *47*, 3045–3051.

(25) Montalti, M.; Cantelli, A.; Battistelli, G. Nanodiamonds and silicon quantum dots: ultrastable and biocompatible luminescent nanoprobes for long-term bioimaging. *Chem. Soc. Rev.* **2015**, *44*, 4853−4921.
(26) Dasog, M.; Kehrle, J.; Rieger, B.; Veinot, J. G. C. Silicon Nanocrystals and Silicon-Polymer Hybrids: Synthesis, Surface Engineering, and Applications. *Angew. Chem., Int. Ed.* **2016**, *55*, 2322−2339.
(27) He, Y.; Fan, C.; Lee, S.-T. Silicon nanostructures for bioapplications. *Nano Today* **2010**, *5*, 282−295.
(28) Wai, C. M.; Hutchison, S. G. Free energy minimization calculation of complex chemical equilibria. Reduction of silicon dioxide with carbon at high temperature. *J. Chem. Educ.* **1989**, *66*, 546−549.
(29) Wu, S.; Zhong, Y.; Zhou, Y.; Song, B.; Chu, B.; Ji, X.; Wu, Y.; Su, Y.; He, Y. Biomimetic Preparation and Dual-Color Bioimaging of Fluorescent Silicon Nanoparticles. *J. Am. Chem. Soc.* **2015**, *137*, 14726−14732.
(30) Zhang, J.; Yu, S.-H. Highly photoluminescent silicon nanocrystals for rapid, label-free and recyclable detection of mercuric ions. *Nanoscale* **2014**, *6*, 4096−4101.
(31) Zhu, J.; Yu, Z.; Burkhard, G. F.; Hsu, C. M.; Connor, S. T.; Xu, Y.; Wang, Q.; McGehee, M.; Fan, S.; Cui, Y. Optical Absorption Enhancement in Amorphous Silicon Nanowire and Nanocone Arrays. *Nano Lett.* **2009**, *9*, 279−282.
(32) Morales, A. M.; Lieber, C. M. A laser ablation method for the synthesis of crystalline semiconductor nanowires. *Science* **1998**, *279*, 208−211.
(33) Heintz, A. S.; Fink, M. J.; Mitchell, B. S. Mechanochemical synthesis of blue luminescent alkyl/alkenyl-passivated silicon nanoparticles. *Adv. Mater.* **2007**, *19*, 3984−3988.
(34) Mangolini, L.; Kortshagen, U. Plasma-assisted synthesis of silicon nanocrystal inks. *Adv. Mater.* **2007**, *19*, 2513−2519.
(35) Arul Dhas, N.; Raj, C. P.; Gedanken, A. Preparation of Luminescent Silicon Nanoparticles: A Novel Sonochemical Approach. *Chem. Mater.* **1998**, *10*, 3278−3281.
(36) Zhong, Y.; Peng, F.; Bao, F.; Wang, S.; Ji, X.; Yang, L.; Su, Y.; Lee, S.-T.; He, Y. Large-Scale Aqueous Synthesis of Fluorescent and Biocompatible Silicon Nanoparticles and Their Use as Highly Photostable Biological Probes. *J. Am. Chem. Soc.* **2013**, *135*, 8350−8356.
(37) Erogbogbo, F.; Yong, K. T.; Roy, I.; Xu, G.; Prasad, P. N.; Swihart, M. T. Biocompatible Luminescent Silicon Quantum Dots for Imaging of Cancer Cells. *ACS Nano* **2008**, *2*, 873−878.
(38) Li, Q.; Luo, T.-Y.; Zhou, M.; Abroshan, H.; Huang, J.; Kim, H. J.; Rosi, N. L.; Shao, Z.; Jin, R. Silicon Nanoparticles with Surface Nitrogen: 90% Quantum Yield with Narrow Luminescence Bandwidth and the Ligand Structure Based Energy Law. *ACS Nano* **2016**, *10*, 8385−8393.
(39) Adam, F.; Appaturi, J. N.; Iqbal, A. The utilization of rice husk silica as a catalyst: Review and recent progress. *Catal. Today* **2012**, *190*, 2−14.
(40) Bakar, R. A.; Yahya, R.; Gan, S. N. Production of High Purity Amorphous Silica from Rice Husk. *Procedia Chem.* **2016**, *19*, 189−195.
(41) Bansal, V.; Ahmad, A.; Sastry, M. Fungus-Mediated Biotransformation of Amorphous Silica in Rice Husk to Nanocrystalline Silica. *J. Am. Chem. Soc.* **2006**, *128*, 14059−14066.
(42) Praneetha, S.; Murugan, A. V. Development of Sustainable development of sustainable rapid microwave assisted process for extg. nanoporous Si from earth abundant agricultural residues and their carbon-based nanohybrids for lithium energy storage. *ACS Sustainable Chem. Eng.* **2015**, *3*, 224−236.
(43) Kim, K. H.; Lee, D. J.; Cho, K. M.; Kim, S. J.; Park, J.-K.; Jung, H.-T. Complete magnesiothermic reduction reaction of vertically aligned mesoporous silica channels to form pure silicon nanoparticles. *Sci. Rep.* **2015**, *5*, 9014.
(44) Holmes, J. D.; Ziegler, K. J.; Doty, R. C.; Pell, L. E.; Johnston, K. P.; Korgel, B. A. Highly Luminescent Silicon Nanocrystals with Discrete Optical Transitions. *J. Am. Chem. Soc.* **2001**, *123*, 3743−3748.
(45) He, Y.; Zhong, Y.-L.; Peng, F.; Wei, X.-P.; Su, Y.-Y.; Lu, Y.-M.; Su, S.; Gu, W.; Liao, L.-S.; Lee, S.-T. One-Pot Microwave Synthesis of Water-Dispersible, Ultraphoto- and pH-Stable, and Highly Fluorescent Silicon Quantum Dots. *J. Am. Chem. Soc.* **2011**, *133*, 14192−14195.
(46) Li, Q.; He, Y.; Chang, J.; Wang, L.; Chen, H.; Tan, Y.-W.; Wang, H.; Shao, Z. Surface-Modified Silicon Nanoparticles with Ultrabright Photoluminescence and Single-Exponential Decay for Nanoscale Fluorescence Lifetime Imaging of Temperature. *J. Am. Chem. Soc.* **2013**, *135*, 14924−14927.
(47) Zhong, Y.; Sun, X.; Wang, S.; Peng, F.; Bao, F.; Su, Y.; Li, Y.; Lee, S.-T.; He, Y. Facile, Large-Quantity Synthesis of Stable, Tunable-Color Silicon Nanoparticles and Their Application for Long-Term Cellular Imaging. *ACS Nano* **2015**, *9*, 5958−5967.
(48) Gather, M. C.; Kohnen, A.; Meerholz, K. White organic light-emitting diodes. *Adv. Mater.* **2011**, *23*, 233−248.
(49) Wang, J.; Lin, W.; Li, W. Three-channel fluorescent sensing via organic white light-emitting dyes for detection of hydrogen sulfide in living cells. *Biomaterials* **2013**, *34*, 7429−7436.
(50) Mukherjee, S.; Thilagar, P. Organic white-light emitting materials. *Dyes Pigm.* **2014**, *110*, 2−27.
(51) Chen, J.; Zhao, D.; Li, C.; Xu, F.; Lei, W.; Sun, L.; Nathan, A.; Sun, X. W. All Solution-processed Stable White Quantum Dot Light-emitting Diodes with Hybrid ZnO@TiO2 as Blue Emitters. *Sci. Rep.* **2015**, *4*, 4085.
(52) Baksi, A.; Mitra, A.; Mohanty, J. S.; Lee, H.; De, G.; Pradeep, T. Size Evolution of Protein-Protected Gold Clusters in Solution: A Combined SAXS-MS Investigation. *J. Phys. Chem. C* **2015**, *119*, 2148−2157.
(53) Zhu, S.; Meng, Q.; Wang, L.; Zhang, J.; Song, Y.; Jin, H.; Zhang, K.; Sun, H.; Wang, H.; Yang, B. Highly Photoluminescent Carbon Dots for Multicolor Patterning, Sensors, and Bioimaging. *Angew. Chem., Int. Ed.* **2013**, *52*, 3953−3957.
(54) Qu, S.; Wang, X.; Lu, Q.; Liu, X.; Wang, L. A Biocompatible Fluorescent Ink Based on Water-Soluble Luminescent Carbon Nanodots. *Angew. Chem., Int. Ed.* **2012**, *51*, 12215−12218.

DOI: 10.1021/acssuschemeng.7b04911
ACS Sustainable Chem. Eng. 2018, 6, 6203−6210